RESEARCH

Autophagy-mediated degradation of NOTCH1 intracellular domain controls the epithelial to mesenchymal transition and cancer metastasis

Sahib Zada[1,2], Jin Seok Hwang[1], Trang Huyen Lai[1], Trang Minh Pham[1], Mahmoud Ahmed[1], Omar Elashkar[1], Wanil Kim[1] and Deok Ryong Kim[1*]

Abstract

Backgound: Autophagy controls levels of cellular components during normal and stress conditions; thus, it is a pivotal process for the maintenance of cell homeostasis. In cancer, autophagy protects cells from cancerous transformations that can result from genomic instability induced by reactive oxygen species or other damaged components, but it can also promote cancer survival by providing essential nutrients during the metabolic stress condition of cancer progression. However, the molecular mechanism underlying autophagy-dependent regulation of the epithelial to mesenchymal transition (EMT) and metastasis is still elusive.

Methods: The intracellular level of NOTCH1 intracellular domain (NICD) in several cancer cells was studied under starvation, treatment with chloroquine or ATG7-knockdown. The autophagy activity in these cells was assessed by immunocytochemistry and molecular analyses. Cancer cell migration and invasion under modulation of autophagy were determined by in vitro scratch and Matrigel assays.

Results: In the study, autophagy activation stimulated degradation of NICD, a key transcriptional regulator of the EMT and cancer metastasis. We also found that NICD binds directly to LC3 and that the NICD/LC3 complex associates with SNAI1 and sequestosome 1 (SQSTM1)/p62 proteins. Furthermore, the *ATG7* knockdown significantly inhibited degradation of NICD under starvation independent of SQSTM1-associated proteasomal degradation. In addition, NICD degradation by autophagy associated with the cellular level of SNAI1. Indeed, autophagy inhibited nuclear translocation of NICD protein and consequently decreased the transcriptional activity of its target genes. Autophagy activation substantially suppressed in vitro cancer cell migration and invasion. We also observed that NICD and SNAI1 levels in tissues from human cervical and lung cancer patients correlated inversely with expression of autophagy-related proteins.

Conclusions: These findings suggest that the cellular level of NICD is regulated by autophagy during cancer progression and that targeting autophagy-dependent NICD/SNAI1 degradation could be a strategy for the development of cancer therapeutics.

*Correspondence: drkim@gnu.ac.kr
[1] Department of Biochemistry and Convergence Medical Science,
Institute of Health Sciences, Gyeongsang National University College
of Medicine, Jinju, Republic of Korea
Full list of author information is available at the end of the article

Zada *et al. Cell & Bioscience*   (2022) 12:17

Page 2 of 15

Background

Autophagy is a catabolic process in which intracellular proteins and organelles are engulfed into double membrane autophagosomes and subsequently fused with lysosomes for degradation. This phenomenon occurs intrinsically to support cell survival in metabolically deficient microenvironments [1–3]. Autophagy plays a context-dependent role in tumorigenesis as a tumor suppressor or a tumor promoter. In normal cells, autophagy maintains genomic stability by removing damaged organelles and proteins, which lead to production of toxic components, such as reactive oxygen species (ROSs). Therefore, dysregulation of autophagy associates closely with cancer occurrence. Autophagy also promotes cancer cell survival during unfavorable metabolic conditions by supplying essential nutrients through the self-eating process [4, 5]. However, the role of autophagy in cancer progression is still debatable.

Metastatic cancer cells migrate from a primary site where cancer has fully developed to distant locations where cancer cells form new colonies, and during this migration, cancer cells must overcome barriers, such as oxidative and metabolic stresses, to reach their destination alive [4, 6]. Metastasis is divided into several distinct steps: detachment from primary tumor tissue, the epithelial to mesenchymal transition (EMT), migration through blood or lymph vessels, invasion into stromal tissue, local crawling, and eventually cell proliferation at the secondary sites [7, 8]. The EMT is an essential initiation step for cancer metastasis and is characterized by the loss of epithelial properties and the gain of mesenchymal characteristics, including increased cell mobility and resistance to apoptosis [7, 9].

The EMT is regulated by several essential oncogenic proteins. In particular, SNAI1 represses gene expression of E-cadherin, an epithelial marker, and promotes expression of mesenchymal proteins, such as N-cadherin, ZEB1/2, and Twist [7, 10, 11]. In addition, NOTCH1 intracellular C-terminal domain (NICD) plays a crucial role in transcriptional activation of EMT mediators, including SNAI1, ZEB1, and N-cadherin [12–14]. Indeed, targeted inhibition of NOTCH1 signaling leads to suppression of cancer progression in many cancer cells [15–17]. Further, it has been suggested that NICD may be targeted for autophagy during cell development and that modulation of SNAI1 during autophagy suppresses cancer progression [18–20]. Previously, we showed that SNAI1 is degraded by starvation-induced autophagy through direct interaction with LC3 [21], and

it has been suggested that autophagy involves regulation of NOTCH1 signaling [22]. Additionally, proteasomal degradation of NICD regulates a variety of cellular processes [23–26]. Further, NICD transcriptional activity has been associated with sequestosome 1 (SQSTM1)/p62, a key autophagy adaptor protein [27, 28]. Nevertheless, the interplay between autophagy and cancer mediators remains elusive because autophagy in cancer cells is highly dynamic and context-dependent.

In this study, we showed that autophagy regulates the intracellular level of NICD through physical and functional interactions with SQSTM1/p62 and LC3 in cancer cells. We also linked NICD with autophagy-dependent degradation of SNAI1. These results suggest that the cancer mediators NICD and SNAI1 may be coordinately regulated by autophagy, and targeting autophagy has potential as an anti-cancer therapeutic strategy.

Materials and methods

Reagents

Dulbecco's modified Eagle's medium (DMEM, 11995-065), Roswell Park Memorial Institute 1640 Medium (RPMI-1640 (11875-119), Hank's buffered saline solution (HBSS, 14025-092) and fetal bovine serum (FBS; 16000-044) were purchased from Gibco and Life Technologies. Chloroquine (C6628) was purchased from Sigma-Aldrich (St. Louis, MO, USA). Rapamycin (R-5000) and Bafilomycin A1 were purchased from LC Laboratories. Anti-FLAG M2 Affinity Gel (lot# SLCD9431) was obtained from Sigma-Aldrich. Glutathione Sepharose 4B beads (Lot#291477) were purchased from Amersham Biosciences. Pierce IP lysis buffers (ref# 8788) were purchased from Thermo Scientific. Primary antibodies against LC3A/B (#12741), SNAIL1 (#3879), NICD (#4147), NOTCH1 (#3608), TCF8/ZEB1 (#3396), N-cadherin (#13116), SQSTM1 (#5114), phospho-ULK1 (Ser555; #5869), phospho-ULK1 (Ser757; #14202), AMPKα (#2532), AMPKα T172 (#2531), MTOR (#2983), phospho-MTOR (Ser2448; #2971) were from Cell Signaling Technology. Primary antibodies against MAP1LC3β (SC-376404), SQSTM1/p62 (SC-28359), Vimentin (SC-6601), E-cadherin (SC-7870), α-Tubulin (SC-5286), and APG7 (SC-376212) were from Santa Cruz Biotechnology, and primary antibody against β-actin (A5441) was from Sigma-Aldrich. Secondary antibodies against rabbit IgG (STAR208P) and mouse IgG (STAR117P) were purchased from Bio-Rad. FITC and TRITC secondary antibodies for immunocytochemistry and Protein A/G PLUS-agarose immunoprecipitation reagent (SC-2003) were purchased

Zada *et al. Cell & Bioscience*   (2022) 12:17

Page 3 of 15

from Santa Cruz Biotechnology. Matrigel (Corning # 344235), propidium iodide (PI), and ProLong Diamond antifade mountant with DAPI (# p36966) were purchased from Invitrogen. SQSTM1 siRNA (29679) was purchased from Santa Cruz Biotechnology, and the NOTCH1 shRNA plasmid was obtained from Sigma-Aldrich.

Cells and cancer tissues

H1299, HeLa and A549 cell lines were obtained from the American Type Culture Collection. HeLa and YCC cells were cultured in DMEM medium (Gibco) with 10% FBS. H1299 and A549 cells were cultured in RPMI-1640 medium (Gibco) with 10 % FBS. All cells were grown at 37 °C in a humidified incubator under 95% air and 5% CO_2. YCC cell lines were established from the ascites and peripheral blood of patients with advanced gastric cancer by the Cancer Metastasis Research Center at Younsei University College of Medicine (Seoul, Korea) as described previously [14, 29, 30]. Cancer and normal tissues from cervical and gastric cancer patients at the Hospital of Gyeongsang National University were used to evaluate protein expression as previously described [14]. This study has been approved by the Institutional Review Board of the Hospital of Gyeongsang National University (IRB #2014-10-024-001).

Cell transfection and Western blot analysis

Hela cells were transiently transfected with pcDNA3.1, FLAG-SNAI1, FLAG-NICD, or FLAG-NICD (1872–2114 a.a) plasmid using Lipofectamine 2000 (Invitrogen). After transfection for 24 h, cells were harvested and lysed using Pierce IP lysis buffer (#87787, Thermo Scientific) supplemented with a protease and phosphatase inhibitor cocktail (Halt^{TM} Protease & phosphatase inhibitor single-use cocktail (100×, Thermo Scientific). Cell extracts were subjected to Western blot or immunoprecipitation analysis. HeLa and H1299 cells were transfected with ATG7 shRNA, siSQSTM, pcDNA, FLAG-NICD, FLAG-SNAI1, shRNA NOTCH1, shRNA control, CRISPR ATG7, or CRISPR control plasmid using Lipofectamine 3000 (Invitrogen) according to the manufacturer's protocol. After incubation for 24 h in fresh medium, cells were starved in HBSS for 4 h and then total proteins were extracted with Pierce IP lysis buffer supplemented with a protease and phosphatase inhibitor cocktail (Halt^{TM} Protease & phosphatase inhibitor single-use cocktail (100×, Thermo Scientific). Protein concentrations were determined with the Pierce protein assay kit (#78440, Thermo Scientific). Total protein lysates (30 μg) were separated by 10% SDS-PAGE and target proteins were detected by Western blotting using the indicated antibodies. Proteins were visualized with the Enhanced Chemiluminescence Detection

Reagent (Thermo Scientific). Each data point was normalized to $β$-actin and the control.

Protein extraction from the human patient tissues

Protein extraction from the human patient tissues was prepared using the protocol described previously [14]. In brief, the minced tissues were homogenized in the RIPA (radioimmunoprecipitation assay) lysis buffer supplemented with a protease and phosphatase inhibitor cocktail (Halt^{TM} Protease & phosphatase inhibitor single-use cocktail (100×, Thermo Scientific), and incubated on ice for 30 min. The protein lysates were centrifuged at 12,000×g for 10 min. Protein concentration was determined with the Pierce protein assay kit (Pierce), and total proteins (30 μg) were used for Western blotting.

Co-immunoprecipation assay

HeLa cells were treated with HBSS for 4 h and lysed using Pierce IP lysis buffer (#87787, Thermo Scientific) supplemented with a protease and phosphatase inhibitor cocktail (Halt^{TM} Protease & phosphatase inhibitor single-use cocktail (100×, Thermo Scientific). Cell lysates were incubated with LC3, SQSTM1, or NICD antibody overnight at 4 °C with gentle rotation. Then, 50 μl G-agarose beads (Santa Cruz, sc11243233001) were added to the antibody mixture and incubated for 4 h with gentle shaking at 4 °C. Immunoprecipitates were washed 3 times, and the bound proteins were eluted by boiling in the 2× SDS loading buffer and subjected to SDS-PAGE. Proteins were detected by Western blotting using the indicated primary antibodies.

Immunohistochemical staining

Cultured cells on coverslips were fixed with 4% (w/v) paraformaldehyde for 30 min and then permeabilized with PBS containing 0.1% Triton X-100 for 20 min at room temperature. Cells were blocked with 5% horse serum in PBS for 1 h and then incubated with primary antibodies overnight at 4 °C. After washing with PBS, cells were incubated with FITC or TRITC-conjugated secondary antibodies (1:50 in PBS) at room temperature for 90 min. Slides were washed twice with PBS for 5 min, and coverslips were mounted using mounting medium containing DAPI. Images were captured by fluorescent microscopy (BX51-DSU; Olympus, Tokyo).

Sub-cellular fractionation

Cultured cells at 70–80% confluency were starved in HBSS medium for 4 h, and then washed with ice-cold PBS. Cells were resuspended in RSB solution (10 mM Tris pH 7.4, 10 mM NaCl, and 6 mM $MgCl_2$) and incubated for 10 min on ice. Then, cells were incubated in RSB with 1 mM DTT, 10 mM NaF, 1 mM $NaVO_4$, and protease/

Zada *et al. Cell & Biosciences*   (2022) 12:17

Page 4 of 15

phosphatase inhibitor cocktail on ice for 15 min. After centrifugation at 14,000 rpm for 30 min, supernatants and pellets were separated as cytosolic and nuclear fractions, respectively. The pellets were resuspended in 3 volumes of buffer C (20% Glycerol, 20 mM HEPES pH 7.9, 420 mM NaCl, and 1.5 mM $MgCl_2$) supplemented with 10 mM NaF, 1 mM NaVO4, and protease/phosphatase inhibitor cocktail and incubated on ice for 30 min.

Luciferase reporter assay
Cells were transfected with the *4XCSL-Luc*, *Hes1-Luc* or *Hes5-Luc* reporter plasmid along with control *renilla-luc* using Lipofectamine 3000. After incubation for 24 h in fresh medium, cells were starved in HBSS for 4 h and then cell lysates were prepared. Firefly and renilla luciferase activities were measured by the Dual-Luciferase Reporter Assay System (Promega). Firefly luciferase activity was normalized to renilla luciferase activity.

Wound-healing assay
Cells were transiently transfected with pcDNA, FLAG-ATG7, or CRISPR/Cas9-Atg7 plasmid and incubated until 100% confluency was reached. Then, cells were starved in HBSS for 4 h. Wounds were scratched into the cell monolayer with a sterile 1000-μL pipette tip in several places. The widths of the wounds were measured using an inverted phase contrast microscope (Nikon, 50× magnification) at 0, 24, 48, and 72 h after scratching. The average distances covered by cells from the initial wound points were determined.

Cell invasion assay
A transwell insert with an 8-μm pore size was used for the two-chamber migration assay. The upper surface of the transwell insert was coated with Matrigel (BD Biosciences; 50 mg/filter). HeLa cells were grown for 24 h and then transiently transfected with pcDNA, FLAG-ATG7, or CRISPR/Cas9-Atg7 plasmid. Cells were starved in HBSS for 4 h. Cells were seeded in serum-free medium in the upper chamber. Serum-containing medium (10% FBS) was placed in the lower chamber as a chemo-attractant. After 36 h, cells that invaded into the bottom surface of the insert were fixed with 3.7% formaldehyde, permeabilized with 100% methanol, and stained with propidium iodide. Cells were photographed under a microscope and quantified by counting numbers of cells in ten randomly selected areas.

Statistical analysis
Each experiment was conducted at least three independent times, and values were expressed as the mean value ± standard deviation (S.D.). Differences between two groups were assessed by the two-tailed student's t-test. One-way Analysis of Variance (ANOVA) was used to compare three groups or more followed by the multiple comparison Tukey's test. Values of *$p < 0.05$ and **$p < 0.01$ were considered significant.

Results

Autophagy promotes NICD degradation in cancer cells
Notch signaling plays a critical role in cell development and differentiation and in control of the EMT and cancer metastasis [14, 25, 31]. To elucidate whether autophagy modulates the intracellular level of NICD, the transcriptional activator domain of NOTCH1, we examined the cellular level of NICD in several cancer cells upon induction of autophagy by starvation or rapamycin treatment. NICD levels were regulated in an autophagy-dependent manner in both HeLa (cervical cancer) and H1299 (lung cancer) cancer cell lines (Fig. 1A–C). Similarly, we previously showed degradation of SNAI1 in autophagy-induced cells [21]. Degradation of both SNAI1 and NICD was inhibited by 20 μM chloroquine, an autophagy inhibitor (Fig. 1A). In addition, YCC (#10) clone, derived from highly metastatic human gastric cancers, exhibited a relatively high expression of NICD among YCC clones according to our previous report [14]. Indeed, the intracellular levels of both NICD and SNAI1 proteins in YCC (#10) cells were also regulated in an autophagy-dependent manner (Additional file 1: Fig. S1). Furthermore, we evaluated autophagy by measuring levels of autophagy markers, including LC3-II, SQSTM1/p62, ULK1 (activatory p-ULK1 at S555 and inhibitory p-ULK1 at S757), and activation of AMP-activated protein kinase (AMPK) and mTOR pathways (p-AMPK at T172, and p-mTOR at S2448) (Fig. 1D–F). Indeed, activation of autophagy proteins was associated with degradation of NICD and SNAI1 proteins. Inversely, inhibitory signals of autophagy (phosphorylation of ULK1 at S757, activation of mTOR at S2448) were associated with increased intracellular levels of NICD and SNAI1 in all cancer cells tested (Fig. 1, Additional file 1: Fig. S1), indicating that autophagy modulates the cellular levels of NICD and SNAI1 proteins, thereby controlling transcriptional activation of several oncogenes essential for EMT and cancer metastasis.

NICD forms protein complexes with LC3, SQSTM1/p62, and SNAI1 during autophagy
In general, membrane-bound LC3 proteins selectively sequester target proteins into the autophagosome lumen through specific interaction with a conserved domain of target proteins called the LC3-interacting region (LIR) [32, 33]. Therefore, selective autophagy is achieved by direct interaction between LC3 and a target protein or indirect interaction between LC3 and a SQSTM1-bound
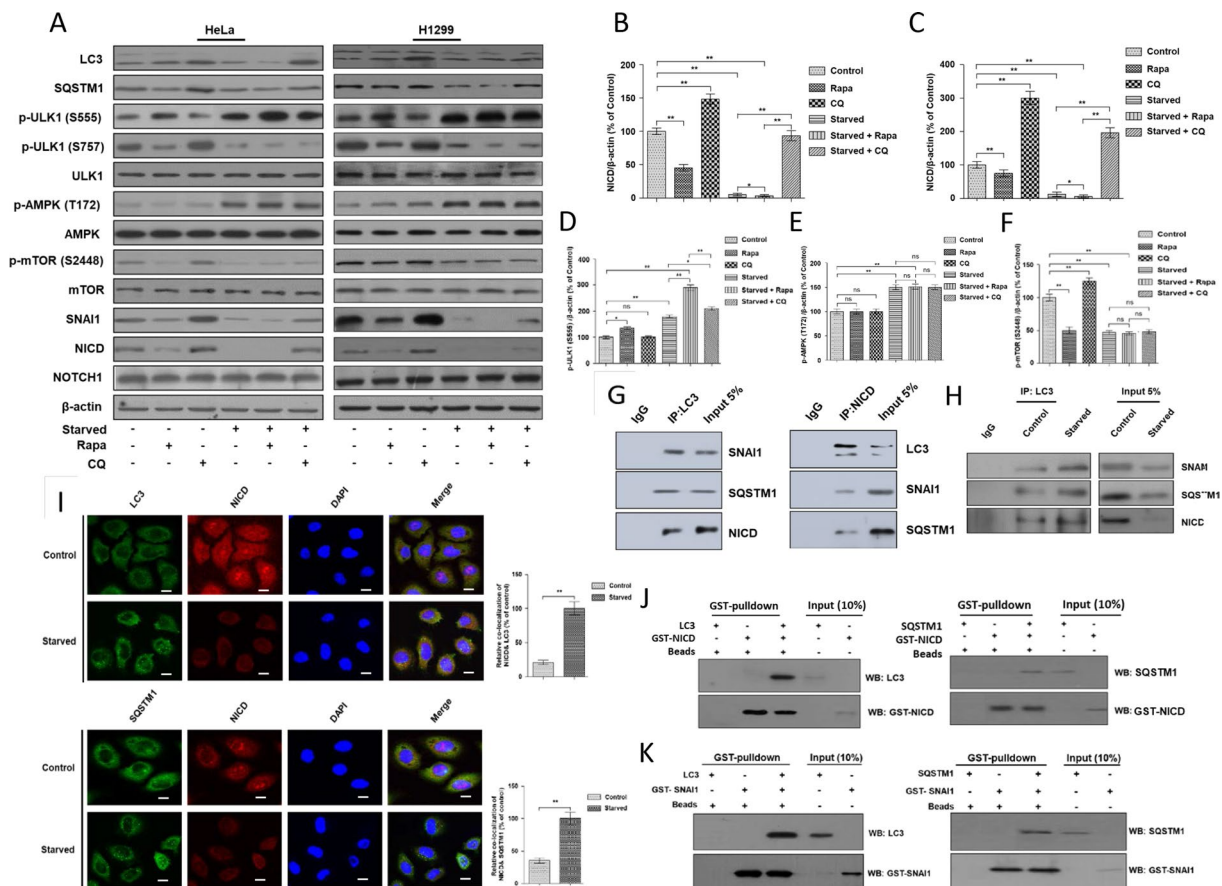
Fig. 1 Autophagy activation stimulates NICD degradation in cancer cells. **A** HeLa and H1299 cells were treated with 100 nM rapamycin (Rapa) or starved in HBSS medium for 4 h in the presence or absence of 20 μM chloroquine (CQ). Total cell extracts (30 μg) were separated by 10% SDS-PAGE and analyzed by Western blotting using primary antibodies against LC3, SQSTM1, p-ULK1-S555, p-ULK1-S757, p-AMPK-T172, AMPK, p-mTOR-S2248, mTOR, SNAI1, NICD, and NOTCH1. *β*-actin was used as the loading control. **B, C** Quantification of NICD cellular levels in cancer cells. The relative protein levels of NICD in HeLa (**B**) and H1299 (**C**) cells, and phosphorylation of ULK at S555 (**D**), AMPK at T172 (**E**) and mTOR at S2448 (**F**) were quantified using NIH ImageJ software. Data represent the mean (± S.D.) of three independent experiments (*P < 0.05 and **P < 0.01). (G) Co-immunoprecipitation. HeLa cell extracts were immunoprecipitated using anti-LC3 (left) or anti-NICD (right) antibodies. The bound proteins were analyzed by Western blotting using the indicated antibody. Whole cell extracts (5% input) were also assessed to control for the amount of total protein. IgG indicates the nonspecific mouse antibody that was used as the negative control. **H** Co-immunoprecipitation in starved cells. Total proteins extracted from starved HeLa cells were immunoprecipitated using anti-LC3 antibodies, and bound proteins were analyzed as described above. **I** Immunocytochemistry. HeLa cells were cultured on coverslips for 24 h and then starved in HBSS for 4 h. After fixing the cells with paraformaldehyde, the cells were incubated for 24 h at 4 °C with two antibodies: LC3 and NICD (top) or SQSTM1 and NICD (bottom). The cells were washed and then incubated with secondary antibodies (FITC-conjugated anti-mouse antibody or TRITC-conjugated anti-rabbit antibody). The coverslips were mounted onto glass slides using a mounting medium containing DAPI, and all images were captured by fluorescence microscopy. Protein colocalization was quantified using NIH Image J software (plugin). Scale bar, 10 μm. Data represent the mean (± S.D.) of three independent experiments (**P < 0.01). **J, K** In vitro interactions between SNAI1 and LC3, SNAI1 and SQSTM1, NICD and LC3, and NICD and SQSTM1. GST-NICD (**J**) or GST-SNAI1 (**K**) proteins were immobilized on glutathione beads and incubated with purified LC3 (left) or SQSTM1 (right) for 1 h at 4 °C. After washing, bound proteins were subjected to 10% SDS-PAGE and visualized by Western blot using anti-LC3, anti-SQSTM1, anti-SNAI1, or anti-NICD

target protein. In the context of selective degradation of NICD by autophagy, we examined the physical interactions between NICD and LC3, SNAI1, and SQSTM1. Based on immunoprecipitation analyses, NICD, LC3, SNAI1, and SQSTM1 proteins likely associate together. Indeed, immunoprecipitation with anti-LC3 antibodies demonstrated the physical association of LC3 with

SNAI1, SQSTM1, and NICD, and immunoprecipitation with anti-NICD antibodies demonstrated the association of NICD with LC3, SNAI1, and SQSTM1 (Fig. 1G). The results were similar for immunoprecipitations with anti-SQSTM1 and anti-SNAI1 (Additional file 1: Fig. S2A, B). The interactions among these proteins increased significantly in starved cells (Fig. 1H and Additional file 1: Fig.

Zada *et al. Cell & Bioscience*   (2022) 12:17

Page 6 of 15

S2C, D). We further assessed interactions among NICD, LC3, SNAI1, and SQSTM1 by immunostaining. NICD co-localized with LC3 and SQSTM1 similarly (Fig. 1I), and SNAI1 co-localized with LC3 and SQSTM1 similarly as with NICD (Additional file 1: Fig. S2E–H). Lastly, we examined the physical interactions between LC3, SQSTM1, NICD, and SNAI1 by in vitro GST-pulldown assays using proteins purified from bacteria (GST-NICD, GST-SNAI1, LC3, SQSTM1). As shown in (Fig. 1J, K), both LC3 and SQSTM1 proteins were pulled down with GST-NICD- and GST-SNAI1-associated glutathione beads. These results indicate that autophagy-induced degradation of NICD and SNAI1 can occur through the LC3- and/or SQSTM1-dependent interaction (Additional file 1: Fig. S2I). Next, we examined the physical interaction between LC3 and NICD proteins containing mutations in putative LIR motifs. By amino acid sequence analysis, we found five putative LIR motifs in NICD (Additional file 1: Fig. S3). Among them, two most conserved LIR motifs (FTPL at 1882 a.a and FQIL at 1976 a.a) in a basis of structural determinants as shown in previous studies were used for LC3 interaction [34–36]. In vitro GST-pulldown assays using bacterially purified GST-NICD and LIR mutant NICD proteins showed that the mutant NICD proteins bound to LC3. Surprisingly, the mutant NICD proteins exhibited very similar interactions with LC3 and SQSTM1 as wild-type NICD (Additional file 1: Fig. S4A, B). In addition, immunoprecipitation with FLAG-NICD and FLAG-SNAI1 showed that NICD complexes with SNAI1 (Additional file 1: Fig. S4C). These results suggest that LC3 interacts dynamically and cooperatively with both NICD and SNAI1 during autophagy-mediated degradation and that the association is not a simple association between LC3 and a single amino acids in an LIR motif in the NICD.

Autophagy-dependent NICD degradation associates with the EMT and cancer metastasis

Proteins involved in the EMT and cancer metastasis are specifically controlled by SNAI1- or NICD-dependent transcriptional regulation. SNAI1 and NICD transcriptionally activate N-cadherin, Zeb1, and Vimentin and suppress E-cadherin during the EMT and metastasis [6, 7, 9]. To investigate the effect of autophagy-dependent NICD degradation on expression of EMT and metastasis genes, we activated or suppressed autophagy by incubating several different cancer cells (HeLa, H1299, A549, and YCC#10 cancer cells) in HBSS medium for 4 h or by treating cells with 20 μM chloroquine, respectively. In all the cancer cells, autophagy was activated upon incubation in HBSS. Activation of ULK1 (phosphorylation at S555 and dephosphorylation at S757) and AMPK (phosphorylation at T172), and a decrease in SQSTM1
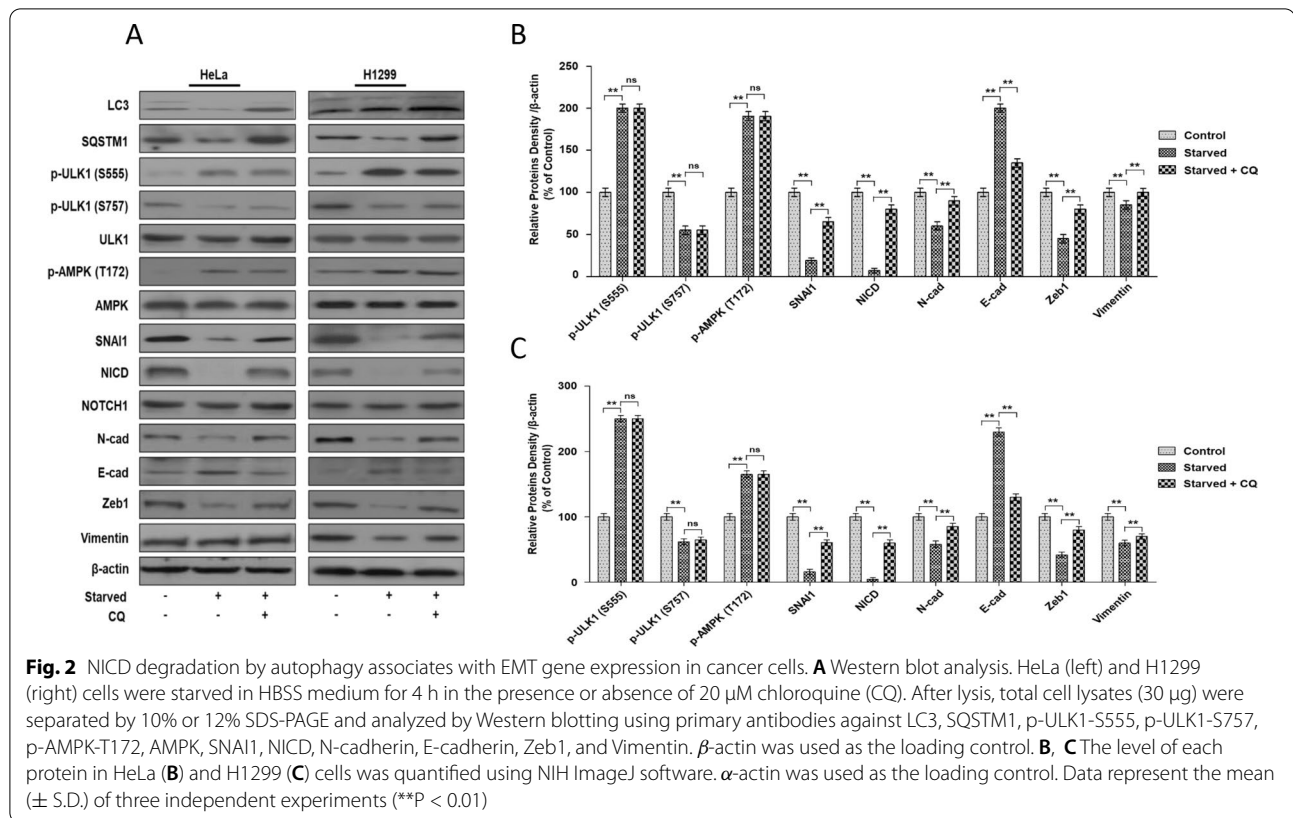
expression were observed upon starvation (Fig. 2A; Additional file 1: Fig. S5). Accordingly, the cellular NICD protein level correlated inversely with autophagy induction, and levels of mesenchymal-related proteins, including N-cadherin, Zeb1, and Vimentin, decreased upon autophagy activation by starvation (Fig. 2; Additional file 1: Fig. S5). By contrast, expression of these proteins increased significantly upon autophagy inhibition with 20 μM chloroquine. E-cadherin expression increased significantly upon autophagy induction by starvation and decreased upon treatment with an autophagy inhibitor (20 μM chloroquine) in all the cancer cell lines (Fig. 2; Additional file 1: Fig. S5). We further assessed NICD expression by immunocytochemistry, and the NICD intensity decreased in starved cancer cells and increased upon treatment with an autophagy inhibitor (Additional file 1: Fig. S6), suggesting that the intracellular level of NICD is regulated specifically by autophagy and associates functionally with transcriptional regulation of EMT and metastasis-related genes during cancer progression.

ATG7 knockdown inhibits starvation-induced NICD degradation

Because autophagy related 7 (ATG7) is a crucial protein in the autophagy process, knockdown of *ATG7* leads to a severe defect in autophagy. To investigate the effect of the *ATG7* genetic knockdown on degradation of NICD, we generated *ATG7*-knockdown cancer cells (HeLa and H1299) using either *ATG7* shRNA or the *ATG7* CRISPR system. As expected, expression of *ATG7* in both HeLa and H1299 cells decreased significantly upon treatment with *ATG7* shRNA, and consequently autophagy was defective and less LC3-II was formed (Fig. 3A). Furthermore, the autophagy defect caused by the *ATG7*-knockdown significantly inhibited degradation of NICD and SNAI1 in starved HeLa and H1299 cancer cells (Fig. 3A–C). In addition, in HeLa and H1299 cells treated with the ATG7 CRISPR system, ATG7 expression decreased significantly and degradation of NICD and SNAI1 was inhibited (Additional file 1: Fig. S7), indicating that ATG7-dependent autophagy controls the levels of NICD and SNAI1 proteins in cancer cells.

NICD degradation is independent of the SQSTM1/p62-associated proteasomal system

SQSTM1/p62 is a classical receptor for selective autophagy, and it has multifunctional roles in autophagy and proteasomal degradation [37–42]. We also showed that SQSTM1 physically and functionally interacts with SNAI1 during autophagy [21]. Here, we examined whether NICD degradation by autophagy requires functional SQSTM1. Surprisingly, we observed substantial degradation of NICD and SNAI1 by starvation-induced

Zada *et al. Cell & Bioscience* (2022) 12:17

Page 7 of 15

Fig. 2 NICD degradation by autophagy associates with EMT gene expression in cancer cells. **A** Western blot analysis. HeLa (left) and H1299 (right) cells were starved in HBSS medium for 4 h in the presence or absence of 20 µM chloroquine (CQ). After lysis, total cell lysates (30 µg) were separated by 10% or 12% SDS-PAGE and analyzed by Western blotting using primary antibodies against LC3, SQSTM1, p-ULK1-S555, p-ULK1-S757, p-AMPK-T172, AMPK, SNAI1, NICD, N-cadherin, E-cadherin, Zeb1, and Vimentin. *β*-actin was used as the loading control. **B**, **C** The level of each protein in HeLa (**B**) and H1299 (**C**) cells was quantified using NIH ImageJ software. *α*-actin was used as the loading control. Data represent the mean (± S.D.) of three independent experiments (**P < 0.01)

autophagy in *SQSTM1*-knockdown cells, although levels of both proteins were slightly higher in *SQSTM1*-knockdown cells than in control cells (Fig. 3D–F). This degradation could result from this and other proteasome degradation systems. Additionally, we examined the effect of proteasomal inhibitor MG-132 on NICD degradation during starvation. As expected, intracellular levels of NICD and SNAI1 proteins decreased during starvation, and this degradation was significantly inhibited by autophagy inhibitor CQ (Fig. 3G–I). However, NICD and SNAI1 were degraded during starvation upon treatment with the proteasome inhibitor MG-132 (Fig. 3G–I) indicating that autophagy-induced degradation of NICD is independent of proteasomal degradation.

Starvation-induced autophagy regulates Notch signaling transcriptional activity and functional association with SNAI1

Because both SNAI1 and Notch signaling play prominent roles in the EMT and cancer metastasis, NOTCH1 and SNAI1 levels may be regulated coordinately and connected functionally during cancer progression. First, we investigated the link between the Notch signal and autophagy-dependent SNAI1 degradation by modulating their expression by knockdown and overexpression.

Surprisingly, the total cellular level of SNAI1 increased significantly in NICD-overexpressing cells and decreased when NICD was downregulated with shRNA-NOTCH1 (Fig. 4A, B). However, overexpression of SNAI1 did not influence the intracellular level of NICD (Fig. 4C, D). Additionally, we examined the SNAI1 level in NOTCH1-knockdown cells upon starvation-induced autophagy (Fig. 4E–G). Interestingly, the cellular level of SNAI1 decreased significantly in NOTCH1-knockdown cells upon starvation. These results indicate that SNAI1 can be degraded via direct interaction with NICD as well as other systems that are independent of Notch signaling.

Because NICD acts as a transcriptional factor, we examined transcriptional activity of NICD upon autophagy induction using three NICD reporter vectors (4XCSL-Luc, Hes1-Luc, and Hes5-Luc) [27]. For all three NICD reporter systems, NICD-induced luciferase reporter activity in HeLa cells decreased significantly upon starvation in HBSS medium, but was restored by inhibition of autophagy with CQ (Fig. 4H, I). We observed similar results in H1299 and A549 cells (Additional file 1: Fig. S8). In addition, we measured relative levels of NICD in the cytosol and nucleus upon starvation in HBSS in the presence or absence of an autophagy inhibitor (20 µM chloroquine). NICD levels in the cytoplasm and nucleus
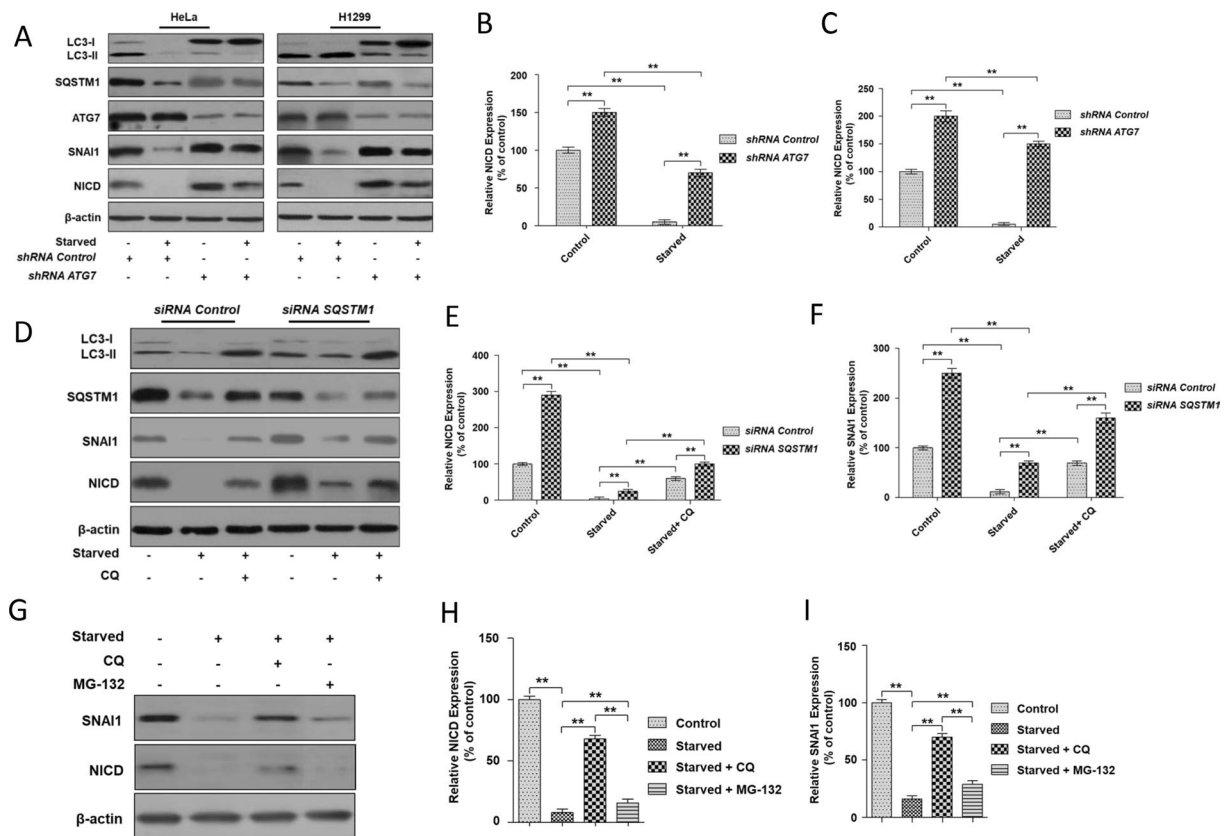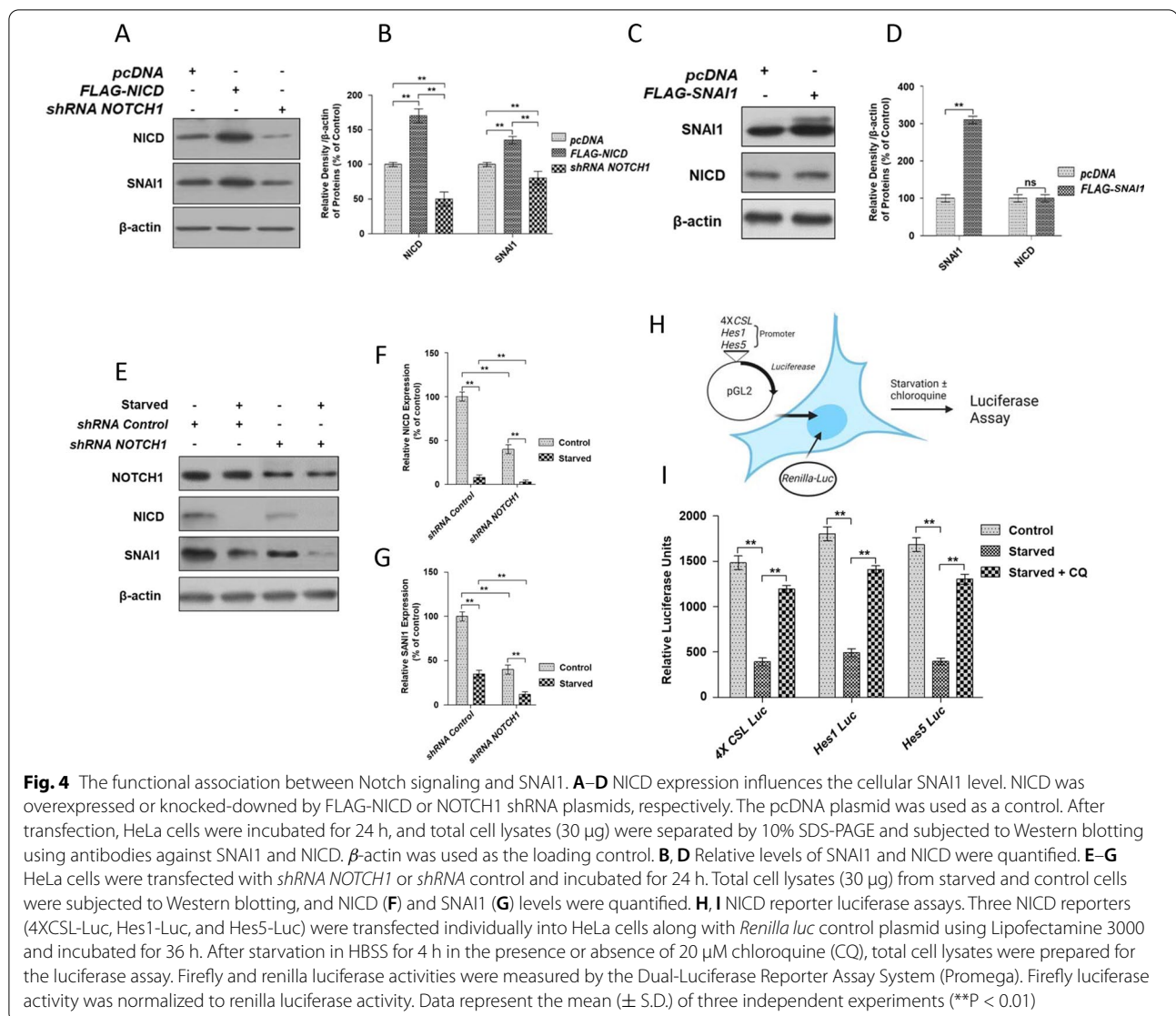
Fig. 3 **A** *ATG7*-knockdown inhibits NICD degradation. HeLa and H1299 cells were transiently transfected with *ATG7* shRNA or control shRNA using Lipofectamine 3000 and incubated for 24 h. Cells were then starved in HBSS for 4 h. Total cell proteins (30 µg) were separated by 10% or 12% SDS-PAGE and analyzed by Western blotting using antibodies against LC3, SQSTM1, ATG7, and SNAI1. *β*-actin was used as the loading control. NICD levels in HeLa cells (**B**) and H1299 cells (**C**) were quantified using NIH ImageJ software. (D) NICD degradation is independent of the SQSTM1-associated proteasome. HeLa cells were transfected with control or *SQSTM1* siRNA using Lipofectamine 3000 and incubated for 24 h. Then, cells were starved in HBSS for 4 h. Total proteins were subjected to Western blotting. Relative levels of NICD (**E**) and SNAI1 (**F**) were quantified. **G** NICD degradation is independent of the proteasomal system. HeLa cells were starved in the presence of either 20 µM chloroquine (CQ) or 20 µM MG-132, and relative levels of NICD (**H**) and SNAI1 (**I**) were quantified. Data represent the mean (± S.D.) of three independent experiments (**P < 0.01)

decreased similarly upon starvation and recovered significantly by the addition of an autophagy inhibitor (Fig. 5A, B). We observed similar autophagic regulation of cytoplasmic and nuclear SNAI1 in this study (Fig. 5A, C) as in a previous study [21]. Furthermore, we assessed nuclear translocation of NICD by immunostaining. Nuclear localization of NICD decreased significantly upon starvation but was rescued by inhibition of autophagy (Fig. 5D). These data indicate that the transcriptional activity of NICD is regulated by autophagy.

The level of NICD in cancer tissues correlates inversely with autophagy activity
To further evaluate the role of autophagy in the EMT and cancer metastasis, we investigated the functional connection between the cellular NICD level and autophagy activity in human cancer tissues and cancer-derived

cells. First, we examined autophagy activity and NICD/ SNAI1 levels in samples from human cervical cancer and lung cancer patients. Interestingly, autophagy activity was lower in cancer tissues and inhibitory phosphorylation of ULK1 (S575) was higher in cancer tissues when compared to normal control tissues. By contrast, activation of autophagy, including activating phosphorylation of ULK1 (S555) and AMPK phosphorylation at T172, and LC3-II formation was lower in both cervical and lung cancer tissues (Fig. 6A). Furthermore, the relative levels of NICD and SNAI1 were higher in cancer tissues than in normal tissues, although there were some variations in autophagy activity (Fig. 6A–C). However, these data suggest that autophagy activity and the cellular NICD level correlate inversely in cancer and normal tissues. We also tested these correlations in several YCC cells derived from human metastatic cancer tissues as described
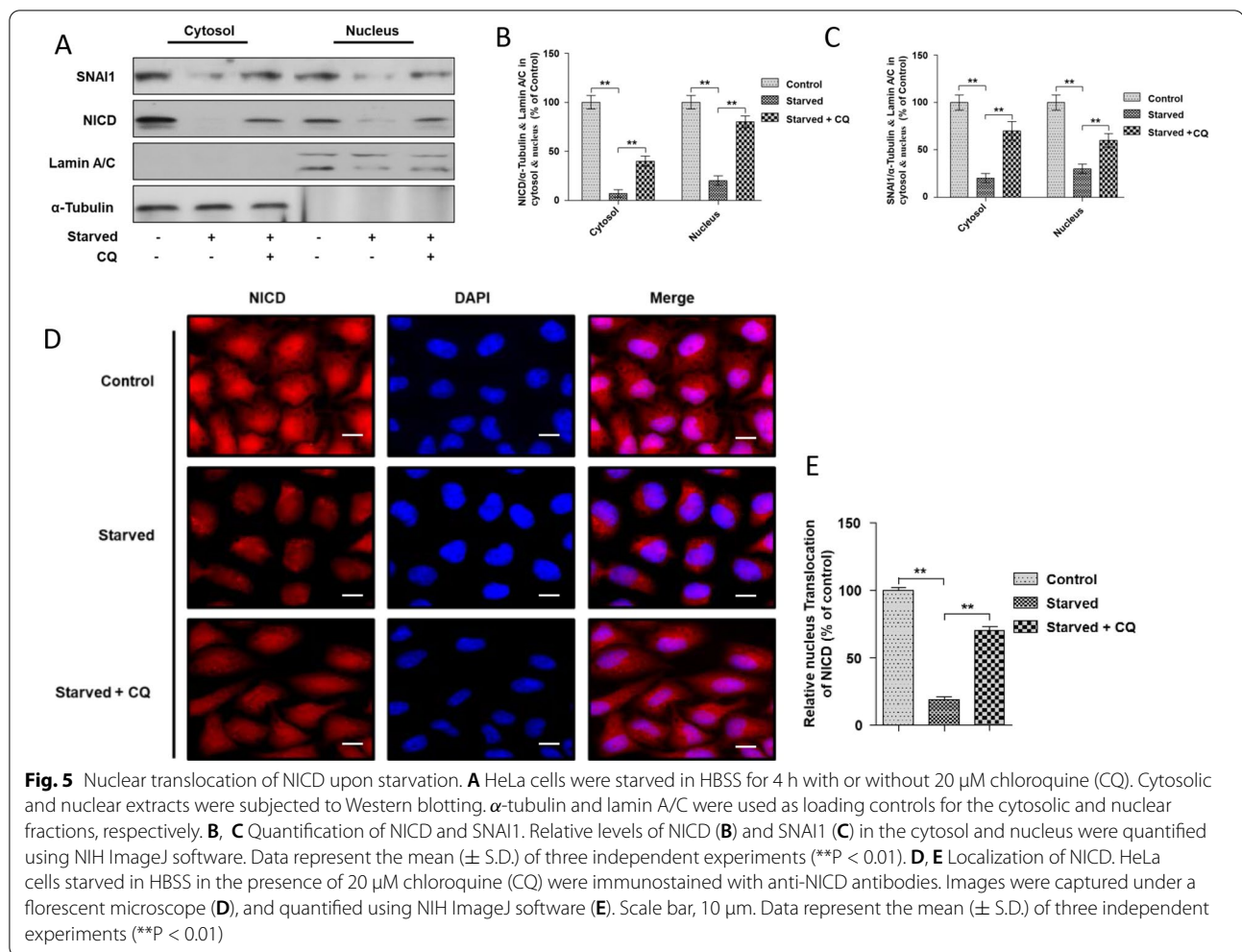
Fig. 4 The functional association between Notch signaling and SNAI1. **A**–**D** NICD expression influences the cellular SNAI1 level. NICD was overexpressed or knocked-downed by FLAG-NICD or NOTCH1 shRNA plasmids, respectively. The pcDNA plasmid was used as a control. After transfection, HeLa cells were incubated for 24 h, and total cell lysates (30 μg) were separated by 10% SDS-PAGE and subjected to Western blotting using antibodies against SNAI1 and NICD. *β*-actin was used as the loading control. **B**, **D** Relative levels of SNAI1 and NICD were quantified. **E**–**G** HeLa cells were transfected with *shRNA NOTCH1* or *shRNA* control and incubated for 24 h. Total cell lysates (30 μg) from starved and control cells were subjected to Western blotting, and NICD (**F**) and SNAI1 (**G**) levels were quantified. **H**, **I** NICD reporter luciferase assays. Three NICD reporters (4XCSL-Luc, Hes1-Luc, and Hes5-Luc) were transfected individually into HeLa cells along with *Renilla luc* control plasmid using Lipofectamine 3000 and incubated for 36 h. After starvation in HBSS for 4 h in the presence or absence of 20 μM chloroquine (CQ), total cell lysates were prepared for the luciferase assay. Firefly and renilla luciferase activities were measured by the Dual-Luciferase Reporter Assay System (Promega). Firefly luciferase activity was normalized to renilla luciferase activity. Data represent the mean (± S.D.) of three independent experiments (**P < 0.01)

previously [14]. Two YCC cells (YCC#10 and YCC#16) exhibited relatively high NICD and SNAI expression and low autophagy activity based on phosphorylation of ULK1 (S555, S757) and AMPK (T172), but the other two YCC cells (YCC#3 and YCC#6) showed an opposite result, low expression of NICD and high activity of autophagy (Additional file 1: Fig. S9A, B), suggesting that the intracellular levels of NICD and SNAI are regulated by autophagy.

Autophagy inhibits NICD-induced migration/invasion of cancer cells

In order to examine how autophagy modulation can exert an influence upon cancer cell migration and

invasion. First, we tested migration of cancer cells using the scratch assay. There was a significant decrease in wound closure activity in starved HeLa cells than in HeLa cells in normal medium (Fig. 6D, E). Furthermore, *ATG7* overexpression in starved cells reduced cell migration severely when compared to the *ATG7* knockdown by CRISPR-*ATG7* (Fig. 6D, E). Also, A459 lung cancer cells displayed similar migration activity as HeLa cervical cancer cells (Additional file 1: Fig. S8C, D). We further examined invasion activity of HeLa cancer cells using the Matrigel chamber assay under the same conditions. Similarly, autophagy induction by *ATG7* overexpression and starvation significantly decreased cancer cell invasion compared to autophagy inhibition by *ATG7* knockdown (Fig. 6F, G). These

Fig. 5 Nuclear translocation of NICD upon starvation. **A** HeLa cells were starved in HBSS for 4 h with or without 20 μM chloroquine (CQ). Cytosolic and nuclear extracts were subjected to Western blotting. α-tubulin and lamin A/C were used as loading controls for the cytosolic and nuclear fractions, respectively. **B**, **C** Quantification of NICD and SNAI1. Relative levels of NICD (**B**) and SNAI1 (**C**) in the cytosol and nucleus were quantified using NIH ImageJ software. Data represent the mean (± S.D.) of three independent experiments (**P < 0.01). **D, E** Localization of NICD. HeLa cells starved in HBSS in the presence of 20 μM chloroquine (CQ) were immunostained with anti-NICD antibodies. Images were captured under a florescent microscope (**D**), and quantified using NIH ImageJ software (**E**). Scale bar, 10 μm. Data represent the mean (± S.D.) of three independent experiments (**P < 0.01)

results indicate that autophagy regulates cancer cell migration and invasion via modulation of intracellular NICD and/or SNAI1.

Discussion

Autophagy has been implicated as a tumor suppressor or cancer promoter depending on the cancer cell type and cellular context [3, 43, 44]. In this study, we suggest that autophagy inhibits cancer progression through intracellular modulation of NICD and SNAI1, key EMT and metastasis regulators. Additionally, autophagy activity correlated inversely with the NICD level and cancer progression in human cancer tissues and several cancer cell lines. Indeed, previous studies indicated that autophagy inhibits cancer cell migration and invasion by regulation of oncogenic proteins SNAI1 and Twist, whereas silencing and knockdown of some autophagy genes restored the mesenchymal phenotypes of cancer cells [20, 21, 45–48]. It has also been suggested that autophagy controls tumor metastasis through regulation of intracellular

NICD levels in cancer cells [18, 19, 22] and that autophagy limits NOTCH1 activity associated with cell differentiation and development [25, 26, 28, 49, 50].

Both NICD and SNAI1 proteins are key regulators of the EMT and cancer metastasis; thus, their intracellular levels are regulated precisely. NICD protein production, which results from Notch signaling, transcriptionally activates to several cancer-promoting proteins, including Slug (Snail homology), N-cadherin, and Zeb1. SNAI1, a transcription factor, inhibits transcriptional activation of some anti-cancer genes, including CDH1/E-cadherin, consequently leading to the EMT, metastasis, and resistance to apoptosis and drugs in most cancers [5, 7, 9, 51, 52]. Also, the Notch1-Snail-E-Cadherin pathway is cooperatively associated with metastatic hepatocellular carcinoma [53], suggesting that the Notch1 signal could transcriptionally activate the SNAI1 gene during EMT and metastasis. In this study, NICD expression decreased significantly upon autophagy activation by starvation and increased upon autophagy inhibition. Furthermore,
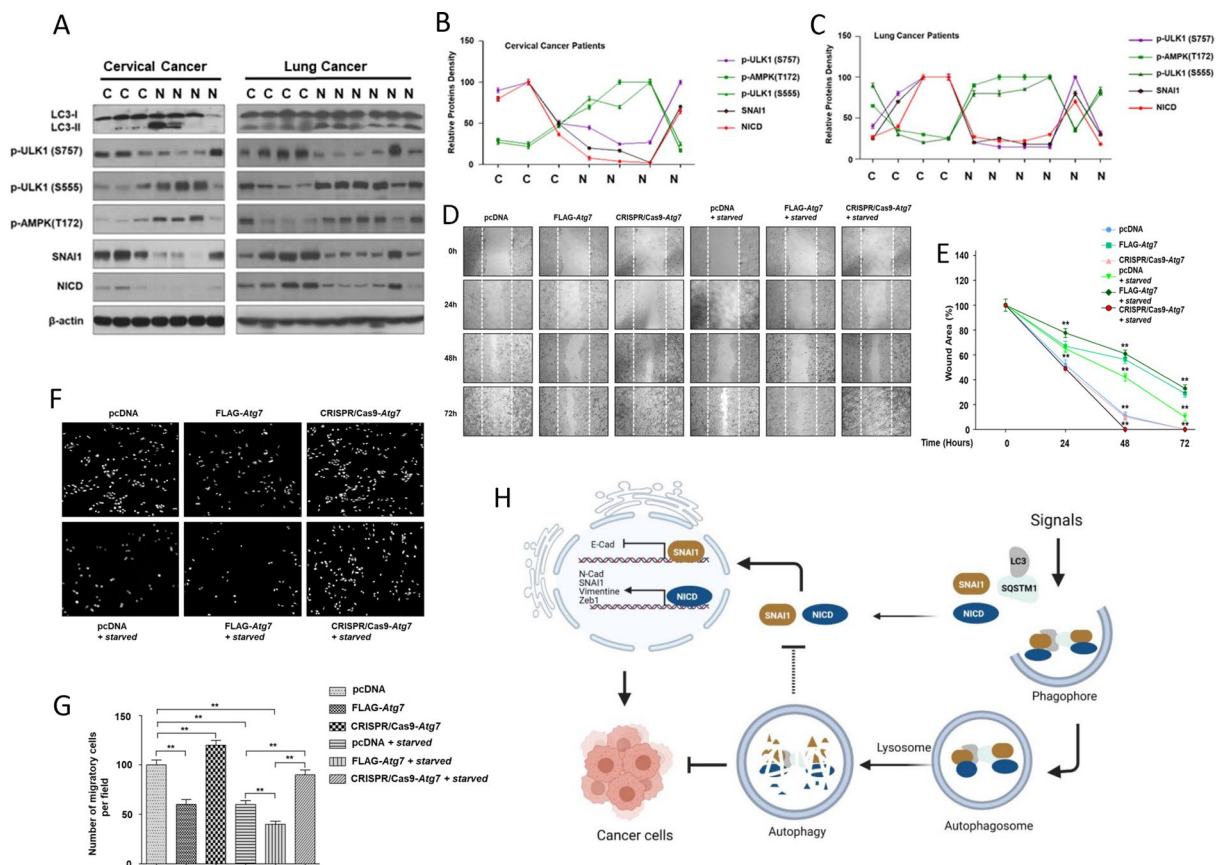
Fig. 6 Correlation between autophagy activity and the NICD level in cancer tissues and the effect of autophagy on cancer cell migration. **A** Total lysates from cancer tissues from cervical (left) and lung (right) cancer patients were prepared. Total protein (30 μg) from each sample (C, cancer tissue; N, normal tissue) was separated by 10% and 12% SDS-PAGE and analyzed by Western blotting using primary antibodies against LC3 ATG5, ATG12, ATG7 p-ULK1-S555, p-ULK1-S757, p-AMPK-T172, SNAI1, and NICD. *β*-actin was used as the loading control. Expression levels of autophagy proteins (p-ULK1-S555, p-ULK1-S757, p-AMPK-T172) and EMT mediators (NICD, SNAI1) in cervical (**B**) and lung (**C**) cancer tissues were quantified using NIH ImageJ software. Data represent the mean (± S.D.) of three independent experiments (**P < 0.01) (**D**) Migration assay. Confluent HeLa cells were pre-treated under various conditions (control, rapamycin, Bafilomycin A1, starvation in HBSS, and combinations of these conditions) for 4 h, and then the confluent layer was scratched using a blue tip. Cells were continuously incubated under the same conditions for 24, 48, or 72 h. At each timepoint, cell migration images (50× magnification) were captured by microscopy. Wound closures (percentage of the average migratory distance of cells relative to the original wound edge) were quantified **E**. Data represent the mean (± S.D.) of at least three independent experiments (**P < 0.01). **F** Matrigel invasion assay. HeLa cells were transiently transfected with pcDNA, FLAG-ATG7, or CRISPR-Cas9-ATG7 plasmids using Lipofectamine 3000 and incubated for 24 h. After invasion of the transwell insert, cells were starved in HBSS for 4 h and then stained with propidium iodide. Cell images (**F**) were captured by microscopy (10× objective magnification) and quantified from 10 randomly selected fields (**G**). Data represent the mean (± S.D.) of three independent experiments (**P < 0.01). **H** A schematic representation of autophagy-dependent NICD degradation during cancer progression. Autophagy signals lead to association of NICD and SNAI1 with LC3 and SQSTM1 to sequester complexes into autophagosomes for degradation. Consequently, nuclear translocation of NICD and SNAI1 is decreased causing transcriptional suppression of EMT-related genes (*N-cadherin*, *Zeb1*, *Vimentin*) and transcriptional activation of *E-cadherin*. As a result, autophagy-dependent degradation of NICD and SNAI1 plays a critical role in the regulation of cancer progression

the regulation of NICD was functionally linked to the autophagy proteins LC3 and SQSTM1/p62. Indeed, previous studies showed that the C-terminal PEST domain of NICD is ubiquitinylated and selectively degraded via SQSTM1-dependent autophagy [18, 23, 26, 54, 55]. Additionally, we showed that NICD complexed with LC3 and SNAI1 during starvation-induced autophagy in cancer cells suggesting that these metastasis proteins

are regulated coordinately by autophagy during cancer progression. In fact, NOTCH1 interacts directly with SNAI1 and induces its degradation in hepatocarcinoma cells [56]. Modulation of NICD and SNAI1 by autophagy further targets their downstream proteins, including N-cadherin, Zeb1, and Vimentin (Fig. 6H). Moreover, Notch signaling inhibits autophagy in some cells indicating a feedback mechanism between NICD and autophagy

Zada *et al. Cell & Biosciene* (2022) 12:17

Page 12 of 15

[50, 57]. As mentioned above, ubiquitination of NICD is a signal for selective autophagy via p62 conjugation and proteasomal degradation. Indeed, the intracellular NICD level is also controlled by the proteasomal system, which illustrates the dynamism of NICD degradation during cellular processes [24, 50, 58, 59].

During selective autophagy, LC3, a lipidated adaptor on autophagosomes, associates with target proteins via direct interaction with their LIR motifs or via indirect interaction mediated by LIR-SQSTM1 adaptor binding to ubiquitinated target proteins [32, 37–39, 60, 61]. In this study, we showed that NICD binds directly to LC3 in cancer cells. Interestingly, even though NICD proteins possess five putative LIR motifs, mutations in two putative LIRs among them did not significantly affect cellular NICD degradation. Based on previous structural studies [34–36], these two LIR motifs of NICD at 1882 a.a (DGFTPL) and at 1976 a.a (GVFQIL) used for LC3 or SQSTM1 interaction are highly conserved in the LIR consensus sequences [(W/F/Y)xx(L/I/V)]. However, we observed that NICD physically interacts with LC3 in our assays suggesting that there may be another unknown protein or interaction that links NICD and LC3. In fact, it was shown that NICD associates with SQSTM1/p62, which suggests that NICD can be removed indirectly by SQSTM1 upon autophagy. It is possible that NICD may require additional partners that can be simultaneously regulated by autophagy. Based on our results, NICD forms a multi-protein complex with SNAI1, LC3, and SQSTM1 during autophagy, and this complex is necessary for autophagy-dependent degradation of NICD during cancer metastasis. Furthermore, the intracellular level of SNAI1 protein can be regulated by selective autophagy via direct interaction with LC3 during cancer progression [21]. Notch signaling also functionally associates with SNAI1 transcriptional activity [25, 53, 56]. Taken together, control of NICD levels in cancer cells may be coordinated with SNAI1 degradation.

In addition, activation of autophagy in cancer cells and tissues correlates inversely with the intracellular NICD level. Some human YCC cancer cell lines that were recently established from cervical and lung cancer tissues from human cancer patients exhibited high levels of NICD [14]. In this study, NICD and SNAI1 levels associated negatively with autophagy activation suggesting that cellular levels of these metastasis regulators could be regulated by autophagy in cancer. In fact, modulation of autophagy by chemical inhibitors, such as CQ or *Atg7* gene knockdown, affect in vitro cancer cell migration. Autophagy activity in cancer is double-edged and depends on the stage and context. Thus, some autophagy inhibitors, including CQ and HCQ, can be used as anti-cancer therapeutics in combination with other cancer drugs for the treatment of several types of cancer [62, 63–65]. However, the anti-cancer activities of CQ and HCQ are mainly autophagy-independent [66, 67]. Nevertheless, autophagy activation may influence cancer treatment. In particular, rapamycin, an autophagy activator, is undergoing testing for anti-cancer activity against colorectal cancer and glioblastoma [20, 68]. Rapamycin downregulates cellular levels of SNAI1 and SLUG proteins. Furthermore, other autophagy activators, including metformin and resveratrol, block survival of various cancer cells [69–74]. Although the cellular level of NICD varies among cancer types, it does associate with autophagy activation as shown in this study.

Conclusion

NICD, a key metastasis regulator, is selectively and coordinately degraded by autophagy through direct interaction with SQSTM1 and LC3 in several cancer cell lines, thereby leading to the inhibition of cancer progression. This autophagy-induced degradation of NICD in the cytoplasm consequently inhibits nuclear translocation of NICD and transcriptional activation of many oncogenes involved in cancer cell invasion and migration. NICD regulation by autophagy varies among cancer cell types and sometimes occurs in an SQSTM1-independent manner indicating that autophagy may have the potential to bypass an SQSTM1 defect or the proteosomal system during the degradation of oncogenic proteins. Based on these data, targeting autophagy could be a possible therapeutic strategy for cancers that show a negative correlation between autophagy activity and the SNAI1/NICD level.

Supplementary Information

The online version contains supplementary material available at https://doi.org/10.1186/s13578-022-00752-3.

Additional file 1. Experimental methods: Plasmid construction; Purification of bacterial proteins and GST-pulldown assay; FLAG-tagged protein immunoprecipitation assay. **Fig. S1.** Specific degradation of NICD associated with autophagy in metastatic YCC cancer cells. **Fig. S2.** Interactions between LC3 or SQSTM1/p62 and NICD or SNAI1 during starvation-induced autophagy. **Fig. S3.** LIR motifs in human NICD. **Fig. S4.** Interaction between LC3 and NICD proteins containing mutant LIR

motifs. **Fig. S5.** NICD degradation by autophagy associates with EMT gene expression in cancer cells. **Fig. S6.** Cellular expression of SNAI1 and NICD in starved cells. **Fig. S7.** Starvation-induced NICD and SNAI1 degradation in ATG7-knockdown cancer cells. **Fig. S8.** Transcriptional activity of NICD in autophagy-induced H1299 and A549 cells measured by luciferase assay. **Fig. S9.** Correlation between autophagy activity and the NICD level in cancer-derived cells and the effect of autophagy on cancer cell migration. Supplementary references.

Availability of data and materials
Data sharing not applicable to this article as no datasets were generated or analyzed during the current study.

Declarations

Ethics approval and consent to participate
Cancer and normal tissues from cervical and gastric cancer patients at the Hospital of Gyeongsang National University were used to evaluate protein expression. This study has been approved by the Institutional Review Board of the Hospital of Gyeongsang National University (IRB #2014-10-024-001).

Consent for publication
Not applicable.

Competing interests
The authors declare that they have no competing interests.

Author details
[1]Department of Biochemistry and Convergence Medical Science, Institute of Health Sciences, Gyeongsang National University College of Medicine, Jinju, Republic of Korea. [2]Present Address: Cancer Biology and Immunology Laboratory, College of Dental Medicine, Columbia University Irving Medical Center, New York, NY, USA.

References
1. Mizushima N, Levine B, Cuervo AM, Klionsky DJ. Autophagy fights disease through cellular self-digestion. Nature. 2008;451(7182):1069–75. https://doi.org/10.1038/nature06639.
2. Dikic I, Elazar Z. Mechanism and medical implications of mammalian autophagy. Nat Rev Mol Cell Biol. 2018;19:349–64. https://doi.org/10.1038/s41580-018-0003-4.
3. White E. Deconvoluting the context-dependent role for autophagy in cancer. Nat Rev Cancer. 2012;12:401–10. https://doi.org/10.1038/nrc3262.
4. Lambert AW, Pattabiraman DR, Weinberg RA. Emerging biological principles of metastasis. Cell. 2017;168(4):670–91. https://doi.org/10.1016/j.cell.2016.11.037.
5. Mani SA, Guo W, Liao MJ, Eaton EN, Ayyanan A, Zhou AY, Brooks M, Reinhard F, Zhang CC, Shipitsin M, Campbell LL, Polyak K, Brisken C, Yang J, Weinberg RA. The epithelial–mesenchymal transition generates cells with properties of stem cells. Cell. 2008;133(4):704–15. https://doi.org/10.1016/j.cell.2008.03.027.
6. Yeung KT, Yang J. Epithelial–mesenchymal transition in tumor metastasis. Mol Oncol. 2017;11(1):28–39. https://doi.org/10.1002/1878-0261.12017.
7. Zheng X, Carstens JL, Kim J, Scheible M, Kaye J, Sugimoto H, Wu CC, Lebleu VS, Kalluri R. Epithelial-to-mesenchymal transition is dispensable for metastasis but induces chemoresistance in pancreatic cancer. Nature. 2015;527:525–30. https://doi.org/10.1038/nature16064.
8. Chaffer CL, Weinberg RA. A perspective on cancer cell metastasis. Science. 2011;331(6024):1559–64. https://doi.org/10.1126/science.1203543.
9. Cano A, Pérez-Moreno MA, Rodrigo I, Locascio A, Blanco MJ, Del Barrio MG, Portillo F, Nieto MA. The transcription factor Snail controls epithelial–mesenchymal transitions by repressing E-cadherin expression. Nat Cell Biol. 2000;2(2):76–83. https://doi.org/10.1038/35000025.
10. Wang Y, Shi J, Chai K, Ying X, Zhou B. The role of snail in EMT and tumorigenesis. Curr Cancer Drug Targets. 2014;13(9):963–72. https://doi.org/10.2174/15680096113136660102.
11. Tran DD, Corsa CAS, Biswas H, Aft RL, Longmore GD. Temporal and spatial cooperation of Snail1 and Twist1 during epithelial–mesenchymal transition predicts for human breast cancer recurrence. Mol Cancer Res. 2011;9(12):1644–57. https://doi.org/10.1158/1541-7786.MCR-11-0371.
12. Wang Z, Li Y, Banerjee S, Sarkar FH. Emerging role of Notch in stem cells and cancer. Cancer Lett. 2009;279(1):8–12. https://doi.org/10.1016/j.canlet.2008.09.030.
13. Dufraine J, Funahashi Y, Kitajewski J. Notch signaling regulates tumor angiogenesis by diverse mechanisms. Oncogene. 2008;27(38):5132–7. https://doi.org/10.1038/onc.2008.227.
14. Noh HS, Hah YS, Ha JH, Kang MY, Zada S, Rha SY, Kang SS, Kim HJ, Park JY, Byun JH, Hahm JR, Shin JK, Jeong SH, Lee YJ, Kim DR. Regulation of the epithelial to mesenchymal transition and metastasis by Raf kinase inhibitory protein-dependent Notch activity. Oncotarget. 2016;7(4):4632–46. https://doi.org/10.18632/oncotarget.6728.
15. Harney AS, Lee J, Manus LM, Wang P, Ballweg DM, LaBonne C, Meade TJ. Targeted inhibition of Snail family zinc finger transcription factors by oligonucleotide-Co(III) Schiff base conjugate. Proc Natl Acad Sci USA. 2009;106(33):13667–72. https://doi.org/10.1073/pnas.0906423106.
16. Shih IM, Wang TL. Notch signaling, γ-secretase inhibitors, and cancer therapy. Cancer Res. 2007;67(5):1879–82. https://doi.org/10.1158/0008-5472.CAN-06-3958.
17. Beverly LJ, Felsher DW, Capobianco AJ. Suppression of p53 by Notch in lymphomagenesis: implications for initiation and regression. Cancer Res. 2005;65(16):7159–68. https://doi.org/10.1158/0008-5472.CAN-05-1664.
18. Zhang T, Guo L, Wang Y, Yang Y. Macroautophagy regulates nuclear NOTCH1 activity through multiple p62 binding sites. IUBMB Life. 2018;70(10):985–94. https://doi.org/10.1002/iub.1891.
19. Tao Z, Li T, Ma H, Yang Y, Zhang C, Hai L, Liu P, Yuan F, Li J, Yi L, Tong L, Wang Y, Xie Y, Ming H, Yu S, Yang X. Autophagy suppresses self-renewal ability and tumorigenicity of glioma-initiating cells and promotes Notch1 degradation. Cell Death Dis. 2018;9(11):1063. https://doi.org/10.1038/s41419-018-0957-3.
20. Catalano M, D'Alessandro G, Lepore F, Corazzari M, Caldarola S, Valacca C, Faienza F, Esposito V, Limatola C, Cecconi F, Di Bartolomeo S. Autophagy induction impairs migration and invasion by reversing EMT in glioblastoma cells. Mol Oncol. 2015;9(8):1612–25. https://doi.org/10.1016/j.molonc.2015.04.016.
21. Zada S, Hwang J, Ahmed M, Lai T, Pham T, Kim D. Control of the epithelial-to-mesenchymal transition and cancer metastasis by autophagy-dependent SNAI1 degradation. Cells. 2019;8(2):129. https://doi.org/10.3390/cells8020129.
22. Ahn JS, Ann EJ, Kim MY, Yoon JH, Lee HJ, Jo EH, Lee K, Lee JS, Park HS. Autophagy negatively regulates tumor cell proliferation through phosphorylation dependent degradation of the Notch1 intracellular domain. Oncotarget. 2016;7(48):79047–63. https://doi.org/10.18632/oncotarget.12986.
23. McGill MA, Dho SE, Weinmaster G, McGlade CJ. Numb regulates post-endocytic trafficking and degradation of notch1. J Biol Chem. 2009;284(39):26427–38. https://doi.org/10.1074/jbc.M109.014845.

Zada *et al. Cell & Bioscience*   (2022) 12:17

Page 14 of 15

24. Luo Z, Mu L, Zheng Y, Shen W, Li J, Xu L, Zhong B, Liu Y, Zhou Y. NUMB enhances Notch signaling by repressing ubiquitination of NOTCH1 intracellular domain. J Mol Cell Biol. 2020;12(5):345–58. https://doi.org/10.1093/jmcb/mjz088.

25. Wu X, Fleming A, Ricketts T, Pavel M, Virgin H, Menzies FM, Rubinsztein DC. Autophagy regulates Notch degradation and modulates stem cell development and neurogenesis. Nat Commun. 2016;7:10533. https://doi.org/10.1038/ncomms10533.

26. Dinicolantonio JJ, Mccarty M. Autophagy-induced degradation of Notch1, achieved through intermittent fasting, may promote beta cell neogenesis: implications for reversal of type 2 diabetes. Open Heart. 2019;6(1):001028. https://doi.org/10.1136/openhrt-2019-001028.

27. Saxena MT, Schroeter EH, Mumm JS, Kopan R. Murine Notch homologs (N1–4) undergo presenilin-dependent proteolysis. J Biol Chem. 2001;276(43):40268–73. https://doi.org/10.1074/jbc.M107234200.

28. Ko SH, Apple EC, Liu Z, Chen L. Age-dependent autophagy induction after injury promotes axon regeneration by limiting NOTCH. Autophagy. 2020;16(11):2052–68. https://doi.org/10.1080/15548627.2020.1713645.

29. Kim TM, Jeong HJ, Seo MY, Kim SC, Cho G, Park CH, Kim TS, Park KH, Chung HC, Rha SY. Determination of genes related to gastrointestinal tract origin cancer cells using a cDNA microarray. Clin Cancer Res. 2005;11(1):79–86.

30. Rha SY, Noh SH, Kim TS, Yoo NC, Roh JK, Min JS, Kim BS. Modulation of biological phenotypes for tumor growth and metastasis by target-specific biological inhibitors in gastric cancer. Int J Mol Med. 1999;4(2):203–12. https://doi.org/10.3892/ijmm.4.2.203.

31. Takebe N, Harris PJ, Warren RQ, Ivy SP. Targeting cancer stem cells by inhibiting Wnt, Notch, and Hedgehog pathways. Nat Rev Clin Oncol. 2011;8(2):97–106. https://doi.org/10.1038/nrclinonc.2010.196.

32. Wirth M, Zhang W, Razi M, Nyoni L, Joshi D, O'Reilly N, Johansen T, Tooze SA, Mouilleron S. Molecular determinants regulating selective binding of autophagy adapters and receptors to ATG8 proteins. Nat Commun. 2019;10(1):2055. https://doi.org/10.1038/s41467-019-10059-6.

33. Noh HS, Hah YS, Zada S, Ha JH, Sim G, Hwang JS, Lai TH, Nguyen HQ, Park JY, Kim HJ, Byun JH, Hahm JR, Kang KR, Kim DR. PEBP1, a RAF kinase inhibitory protein, negatively regulates starvation-induced autophagy by direct interaction with LC3. Autophagy. 2016;12(11):2183–96. https://doi.org/10.1080/15548627.2016.1219013.

34. Birgisdottir ÅB, Lamark T, Johansen T. The LIR motif—crucial for selective autophagy. J Cell Sci. 2013;126(Pt 15):3237–47. https://doi.org/10.1242/jcs.126128.

35. Birgisdottir ÅB, Mouilleron S, Bhujabal Z, Wirth M, Sjøttem E, Evjen G, Zhang W, Lee R, O'Reilly N, Tooze SA, Lamark T, Johansen T. Members of the autophagy class III phosphatidylinositol 3-kinase complex I interact with GABARAP and GABARAPL1 via LIR motifs. Autophagy. 2019;15(8):1333–55. https://doi.org/10.1080/15548627.2019.1581009.

36. Johansen T, Lamark T. Selective autophagy: ATG8 family proteins, LIR motifs and cargo receptors. J Mol Biol. 2020;432(1):80–103. https://doi.org/10.1016/j.jmb.2019.07.016.

37. Pankiv S, Clausen TH, Lamark T, Brech A, Bruun JA, Outzen H, Øvervatn A, Bjørkøy G, Johansen T. p62/SQSTM1 binds directly to Atg8/LC3 to facilitate degradation of ubiquitinated protein aggregates by autophagy. J Biol Chem. 2007;282(33):24131–45. https://doi.org/10.1074/jbc.M702824200.

38. Shvets E, Fass E, Scherz-Shouval R, Elazar Z. The N-terminus and Phe52 residue of LC3 recruit p62/SQSTM1 into autophagosomes. J Cell Sci. 2008;121(16):2685–95. https://doi.org/10.1242/jcs.026005.

39. Noda NN, Ohsumi Y, Inagaki F. Atg8-family interacting motif crucial for selective autophagy. FEBS Lett. 2010;584(7):1379–85. https://doi.org/10.1016/j.febslet.2010.01.018.

40. Ichimura Y, Kirisako T, Takao T, Satomi Y, Shimonishi Y, Ishihara N, Mizushima N, Tanida I, Kominami E, Ohsumi M, Noda T, Ohsumi Y. A ubiquitin-like system mediates protein lipidation. Nature. 2000;408:488–92. https://doi.org/10.1038/35044114.

41. Demishtein A, Fraiberg M, Berko D, Tirosh B, Elazar Z, Navon A. SQSTM1/p62-mediated autophagy compensates for loss of proteasome polyubiquitin recruiting capacity. Autophagy. 2017;13(10):1697–708. https://doi.org/10.1080/15548627.2017.1356549.

42. Nihira K, Miki Y, Ono K, Suzuki T, Sasano H. An inhibition of p62/SQSTM1 caused autophagic cell death of several human carcinoma cells. Cancer Sci. 2014;105(5):568–75. https://doi.org/10.1111/cas.12396.

43. Klionsky DJ. Autophagy: from phenomenology to molecular understanding in less than a decade. Nat Rev Mol Cell Biol. 2007;8(11):931–7. https://doi.org/10.1038/nrm2245.

44. White E, DiPaola RS. The double-edged sword of autophagy modulation in cancer. Clin Cancer Res. 2009;15(17):5308–16. https://doi.org/10.1158/1078-0432.CCR-07-5023.

45. Qiang L, Zhao B, Ming M, Wang N, He TC, Hwang S, Thorburn A, He YY. Regulation of cell proliferation and migration by p62 through stabilization of Twist1. Proc Natl Acad Sci USA. 2014;111(25):9241–6. https://doi.org/10.1073/pnas.1322913111.

46. Grassi G, Di Caprio G, Santangelo L, Fimia GM, Cozzolino AM, Komatsu M, Ippolito G, Tripodi M, Alonzi T. Autophagy regulates hepatocyte identity and epithelial-to-mesenchymal and mesenchymal-to-epithelial transitions promoting Snail degradation. Cell Death Dis. 2015;6(9):1880. https://doi.org/10.1038/cddis.2015.249.

47. Gugnoni M, Sancisi V, Gandolfi G, Manzotti G, Ragazzi M, Giordano D, Tamagnini I, Tigano M, Frasoldati A, Piana S, Ciarrocchi A. Cadherin-6 promotes EMT and cancer metastasis by restraining autophagy. Oncogene. 2017;36(5):667–77. https://doi.org/10.1038/onc.2016.237.

48. Lv Q, Wang W, Xue J, Hua F, Mu R, Lin H, Yan J, Lv X, Chen X, Hu ZW. DEDD interacts with PI3KC3 to activate autophagy and attenuate epithelial–mesenchymal transition in human breast cancer. Cancer Res. 2012;72(13):3238–50. https://doi.org/10.1158/0008-5472.CAN-11-3832.

49. Zeng J, Jing Y, Shi R, Pan X, Lai F, Liu W, Li R, Gao L, Hou X, Wu M, Wei L. Autophagy regulates biliary differentiation of hepatic progenitor cells through Notch1 signaling pathway. Cell Cycle. 2016;15(12):1602–10. https://doi.org/10.1080/15384101.2016.1181234.

50. Marcel N, Sarin A. Notch1 regulated autophagy controls survival and suppressor activity of activated murine T-regulatory cells. eLife. 2016;5:14023. https://doi.org/10.7554/eLife.14023.

51. Wang T, Xuan X, Pian L, Gao P, Xu H, Zheng Y, Zang W, Zhao G. Notch-1-mediated esophageal carcinoma EC-9706 cell invasion and metastasis by inducing epithelial–mesenchymal transition through Snail. Tumor Biol. 2014;35(2):1193–201. https://doi.org/10.1007/s13277-013-1159-3.

52. Wang HG. Autophagy and cancer. New York: Springer; 2013. https://doi.org/10.1007/978-1-4614-6561-4.

53. Wang XQ, Zhang W, Lui ELH, Zhu Y, Lu P, Yu X, Sun J, Yang S, Poon RTP, Fan ST. Notch1-Snail1-E-cadherin pathway in metastatic hepatocellular carcinoma. Int J Cancer. 2012;131(3):163–72. https://doi.org/10.1002/ijc.27336.

54. O'Neil J, Grim J, Strack P, Rao S, Tibbitts D, Winter C, Hardwick J, Welcker M, Meijerink JP, Pieters R, Draetta G, Sears R, Clurman BE, Look AT. FBW7 mutations in leukemic cells mediate NOTCH pathway activation and resistance to γ-secretase inhibitors. J Exp Med. 2007;204(8):1813–24. https://doi.org/10.1084/jem.20070876.

55. McGill MA, McGlade CJ. Mammalian Numb proteins promote Notch1 receptor ubiquitination and degradation of the Notch1 intracellular domain. J Biol Chem. 2003;278(25):23196–203. https://doi.org/10.1074/jbc.M302827200.

56. Lim SO, Kim HS, Quan X, Ahn SM, Kim H, Hsieh D, Seong JK, Jung G. Notch1 binds and induces degradation of Snail in hepatocellular carcinoma. BMC Biol. 2011;9:1–12. https://doi.org/10.1186/1741-7007-9-83.

57. Li YJ, Lei YH, Yao N, Wang CR, Hu N, Ye WC, Zhang DM, Chen ZS. Autophagy and multidrug resistance in cancer. Chin J Cancer. 2017. https://doi.org/10.1186/s40880-017-0219-2.

58. Moretti J, Brou C. Ubiquitinations in the Notch signaling pathway. Int J Mol Sci. 2013;14(3):6359–81. https://doi.org/10.3390/ijms14036359.

59. Öberg C, Li J, Pauley A, Wolf E, Gurney M, Lendahl U. The Notch intracellular domain is ubiquitinated and negatively regulated by the mammalian Sel-10 homolog. J Biol Chem. 2001;276(38):35847–53. https://doi.org/10.1074/jbc.M103992200.

60. Birgisdottir ÅB, Lamark T, Johansen T. The LIR motif—crucial for selective autophagy. J Cell Sci. 2013;126(15):3237–47. https://doi.org/10.1242/jcs.126128.

61. Bjørkøy G, Lamark T, Brech A, Outzen H, Perander M, Øvervatn A, Stenmark H, Johansen T. p62/SQSTM1 forms protein aggregates degraded by autophagy and has a protective effect on huntingtin-induced cell death. J Cell Biol. 2005;171(4):603–14. https://doi.org/10.1083/jcb.200507002.

62. Rosenfeld MR, Ye X, Supko JG, Desideri S, Grossman SA, Brem S, Mikkelson T, Wang D, Chang YC, Hu J, McAfee Q, Fisher J, Troxel AB, Piao S, Heitjan DF, Tan KS, Pontiggia L, O'Dwyer PJ, Davis LE, Amaravadi RK. A phase I/

II trial of hydroxychloroquine in conjunction with radiation therapy and concurrent and adjuvant temozolomide in patients with newly diagnosed glioblastoma multiforme. Autophagy. 2014;10(8):1359–68. https://doi.org/10.4161/auto.28984.

63. Amaravadi RK, Yu D, Lum JJ, Bui T, Christophorou MA, Evan GI, Thomas-Tikhonenko A, Thompson CB. Autophagy inhibition enhances therapy-induced apoptosis in a Myc-induced model of lymphoma. J Clin Investig. 2007;117(2):326–36. https://doi.org/10.1172/JCI28833.

64. Vogl DT, Stadtmauer EA, Tan KS, Heitjan DF, Davis LE, Pontiggia L, Rangwala R, Piao S, Chang YC, Scott EC, Paul TM, Nichols CW, Porter DL, Kaplan J, Mallon G, Bradner JE, Amaravadi RK. Combined autophagy and proteasome inhibition a phase 1 trial of hydroxychloroquine and bortezomib in patients with relapsed/refractory myeloma. Autophagy. 2014;10(8):1380–90. https://doi.org/10.4161/auto.29264.

65. ...Rangwala R, Chang YC, Hu J, Algazy KM, Evans TL, Fecher LA, Schuchter LM, Torigian DA, Panosian JT, Troxel AB, Tan KS, Heitjan DF, DeMichele AM, Vaughn DJ, Redlinger M, Alavi A, Kaiser J, Pontiggia L, Davis LE, O'Dwyer PJ, Amaravadi RK. Combined MTOR and autophagy inhibition: phase I trial of hydroxychloroquine and temsirolimus in patients with advanced solid tumors and melanoma. Autophagy. 2014;10(8):1391–402. https://doi.org/10.4161/auto.29119.

66. Maes H, Kuchnio A, Carmeliet P, Agostinis P. Chloroquine anticancer activity is mediated by autophagy-independent effects on the tumor vasculature. Mol Cell Oncol. 2016;3(1):970097. https://doi.org/10.4161/23723548.2014.970097.

67. Maycotte P, Aryal S, Cummings CT, Thorburn J, Morgan MJ, Thorburn A. Chloroquine sensitizes breast cancer cells to chemotherapy independent of autophagy. Autophagy. 2012;8(2):200–12. https://doi.org/10.4161/auto.8.2.18554.

68. Zhang H, Zhang H, Zhang Y, Ng SS, Ren F, Wang Y, Duan Y, Chen L, Zhai Y, Guo Q, Chang Z. Dishevelled-DEP domain interacting protein (DDIP) inhibits Wnt signaling by promoting TCF4 degradation and disrupting the TCF4/β-catenin complex. Cell Signal. 2010;22(11):1753–60. https://doi.org/10.1016/j.cellsig.2010.06.016.

69. Tian Y, Song W, Li D, Cai L, Zhao Y. Resveratrol as a natural regulator of autophagy for prevention and treatment of cancer. OncoTargets Ther. 2019;12:8601–9. https://doi.org/10.2147/OTT.S213043.

70. Wang M, Yu T, Zhu C, Sun H, Qiu Y, Zhu X, Li J. Resveratrol triggers protective autophagy through the ceramide/Akt/mTOR pathway in melanoma B16 cells. Nutr Cancer. 2014;66(3):435–40. https://doi.org/10.1080/01635581.2013.878738.

71. De Santi M, Baldelli G, Diotallevi A, Galluzzi L, Schiavano GF, Brandi G. Metformin prevents cell tumorigenesis through autophagy-related cell death. Sci Rep. 2019;9(1):1–11. https://doi.org/10.1038/s41598-018-37247-6.

72. Mogavero A, Maiorana MV, Zanutto S, Varinelli L, Bozzi F, Belfiore A, Volpi CC, Gloghini A, Pierotti MA, Gariboldi M. Metformin transiently inhibits colorectal cancer cell proliferation as a result of either AMPK activation or increased ROS production. Sci Rep. 2017;7(1):1–12. https://doi.org/10.1038/s41598-017-16149-z.

73. Sesen J, Dahan P, Scotland SJ, Saland E, Dang VT, Lemarié A, Tyler BM, Brem H, Toulas C, Moyal ECJ, Sarry JE, Skuli N. Metformin inhibits growth of human glioblastoma cells and enhances therapeutic response. PLoS ONE. 2015;10(4):1–24. https://doi.org/10.1371/journal.pone.0123721.

74. Lin H, Li N, He H, Ying Y, Sunkara S, Luo L, Lv N, Huang D, Luo Z. AMPK inhibits the stimulatory effects of TGF-β on Smad2/3 activity, cell migration, and epithelial-to-mesenchymal transition. Mol Pharmacol. 2015;88(6):1062–71. https://doi.org/10.1124/mol.115.099549.

Publisher's Note